Journal of Computational Physics 229 (2010) 6676–6687

Contents lists available at ScienceDirect

Journal of Computational Physics

journal homepage: www.elsevier.com/locate/jcp

Short note

Viscous and inviscid regularizations in a class of evolutionary partial differential equations

Roberto Camassa [a], Pao-Hsiung Chiu [b], Long Lee [c,*], Tony W.H. Sheu [d,e]

[a] Department of Mathematics, University of North Carolina, Chapel Hill, North Carolina, USA
[b] Nuclear Engineering Division, Institute of Nuclear Energy Research, Taoyuan County, Taiwan, ROC
[c] Department of Mathematics, University of Wyoming, Laramie, Wyoming, USA
[d] Department of Engineering Science and Ocean Engineering, National Taiwan University, Taipei, Taiwan, ROC
[e] Taida Institute of Mathematical Science (TIMS), National Taiwan University, Taipei, Taiwan, ROC

ARTICLE INFO

Article history:
Received 7 March 2010
Received in revised form 1 June 2010
Accepted 1 June 2010
Available online 9 June 2010

Keywords:
Helmholtz equation
Iterative algorithm
Leray-type regularization
Hopt equation
Regularized Burgers equation

ABSTRACT

We investigate solution properties of a class of evolutionary partial differential equations (PDEs) with viscous and inviscid regularization. An equation in this class of PDEs can be written as an evolution equation, involving only first-order spatial derivatives, coupled with the Helmholtz equation. A recently developed two-step iterative method (P.H. Chiu, L. Lee, T.W.H. Sheu, A dispersion-relation-preserving algorithm for a nonlinear shallow-water wave equation, J. Comput. Phys. 228 (2009) 8034–8052) is employed to study this class of PDEs. The method is in principle superior for PDE's in this class as it preserves their physical dispersive features. In particular, we focus on a Leray-type regularization (H.S. Bhat, R.C. Fetecau, A Hamiltonian regularization of the Burgers equation, J. Nonlinear Sci. 16 (2006) 615–638) of the Hopf equation proposed in alternative to the classical Burgers viscous term. We show that the regularization effects induced by the alternative model can be vastly different from those induced by Burgers viscosity depending on the smoothness of initial data in the limit of zero regularization. We validate our numerical scheme by comparison with a particle method which admits closed form solutions. Further effects of the interplay between the dispersive terms comprising the Leray-regularization are illustrated by solutions of equations in this class resulting from regularized Burgers equation by selective elimination of dispersive terms.

1. Introduction

Members of the class of evolutionary PDEs

$$m_t + Au_x m + Bum_x + Cuu_x + Du_{xxt} = Ku_x, \tag{1.1}$$

where $m = u - \alpha^2 u_{xx}$ is the Helmholtz operator acting on the dependent variable u, function of the spatial variable x and time t, and A, B, C, D, K are constants, have recently attracted intense interest from both a mathematical and physical perspective, following the derivation of a member of this class (also known as the Camassa-Holm (CH) equation), in the context of shallow-water wave dynamics (see e.g. [5,10]). The CH equation

$$u_t + 2\kappa u_x - u_{xxt} + 3uu_x = 2u_x u_{xx} + uu_{xxx}, \tag{1.2}$$

* Corresponding author. Tel.: +1 307 766 4368; fax: +1 307 766 6838.
E-mail address: llee@uwyo.edu (L. Lee).

0021-9991/$ - see front matter © 2010 Elsevier Inc. All rights reserved.
doi:10.1016/j.jcp.2010.06.002

corresponds to the choice of coefficients $A = 2$, $B = 1$, $C = 0$, $D = 0$, $K = -2\kappa$, and $\alpha = 1$ in Eq. (1.1). The limit $\kappa = 0$ in Eq. (1.2) makes it effectively non-dispersive, and its soliton traveling wave solutions become weak solutions with a corner singularity at their peaks (hence the name "peakons" by which they are often referred).

Other equations from this class of PDEs include:

1. $A = 0$, $B = 1$, $C = 0$, $D = 0$, and $K = 0$. This is a "regularized" Burgers equation

$$m_t + um_x = 0. \tag{1.3}$$

This equation and its extensions have attracted some attention in the recent literature. With the definition of the one dimensional Helmholtz operator

$$\mathcal{H} = 1 - \alpha^2 \partial_{xx}, \tag{1.4}$$

and its Green's function, one can represent u in terms of m as:

$$u(x,t) = \frac{1}{2\alpha} \int_{-\infty}^{\infty} \exp(-|x-y|/\alpha) m(y,t) dy. \tag{1.5}$$

The Leray-type [11] smoothed velocity u has been recently proposed for its role of regularizing the inviscid Burgers equation.

$$u_t + uu_x = 0. \tag{1.6}$$

With nonzero viscosity, the Burgers equation

$$u_t + uu_x = vu_{xx} \tag{1.7}$$

is the simplest model combing nonlinear propagation effect and the diffusive effect, while its inviscid version for $v = 0$, also known as Hopf equation, is the simplest model of shock forming hyperbolic equation. In [13,14], attempts were made to compare regularization effects induced by the viscosity and the filtered velocity (1.5). It is well known that one can study the Burgers equation to determine the physically relevant solutions of the Hopf equation. A similar approach has been proposed (see, e.g. [1]) for the solutions of the regularized Burgers Eq. (1.3), written in the form

$$u_t + uu_x = \alpha^2 (u_{xxt} + uu_{xxx}), \tag{1.8}$$

to show that solutions of this equation converge strongly to physically relevant weak solutions of the Hopf Eq. (1.6) as $\alpha \to 0$, provided the initial data $u(x,0)$ are in a suitable function space. Thus, Eq. (1.8) has been proposed as an alternative to Burgers equation (1.6) in this respect. We remark that an alternative viewpoint of Eq. (1.3), closer to that of Leray [11] whose original purpose was to study models of turbulent flows, is to consider $m(x,t)$ as the primary variable, and hence assign initial conditions $m(x,0) = m_0(x)$. Provided the operator (1.4) is invertible on such initial data, this viewpoint is perfectly equivalent to that of regularizing the Hopf equation, but of course the degree of smoothness of the initial data plays a different role with respect to which viewpoint is adopted.

2. $A = 0$, $B = 1$, $C = 0$, $D = \alpha^2$, and $K = 0$. This gives rise to a nonlinear dispersive equation of Korteweg-de Vries (KdV)-type,

$$u_t + um_x = 0, \tag{1.9}$$

or

$$u_t + uu_x = \alpha^2 uu_{xxx}. \tag{1.10}$$

3. $A = 0$, $B = 0$, $C = 1$, $D = 0$, and $K = 0$. This is an equation with the so-called Benjamin–Bona–Mahony (BBM) structure

$$m_t + uu_x = 0, \tag{1.11}$$

or

$$u_t + uu_x = \alpha^2 u_{xxt}. \tag{1.12}$$

It is well known that solutions of this BBM equation fail to converge to weak solutions of the Hopf equation as $\alpha \to 0$.

We notice that all equations in this class have no derivatives of order higher than third explicitly (either $D = 0$, or $D = \alpha^2$ in Eq. (1.1)). All these equations share the formulation of a first-order derivative coupled with the Helmholtz equation. Hence it is natural to introduce a two-step iterative algorithm for this class of PDEs, by solving the first-order equation first and follow this by a solution of the Helmholtz equation, then repeating the process until convergence criteria are satisfied.

The focus of this paper is to employ a higher-order dispersion-relation-preserving two-step algorithm to study a class of PDEs (1.1). We introduce the algorithm in Section 2. We illustrate the solution properties of the regularized Burgers equation (1.3), the dispersive Eq. (1.9), and the BBM Equation (1.11) in Sections 3 and 4.

2. Two-step iterative algorithm

If $D = 0$ in Eq. (1.1), the PDE can be expressed as:

$$m_t = F(m, u, m_x, u_x), \quad m = u - \alpha^2 u_{xx}. \tag{2.1}$$

The evolution equation in (2.1) can be solved by a standard method of lines (MOL). Let $m^n = m(t^n, x)$ and $m^{n+1} = m(t^n + \Delta t, x)$ be the semi-discretized m values at time level n and $n+1$, respectively. The MOL using the midpoint time integrator yields

$$\frac{m^{n+1} - m^n}{\Delta t} = F\left(m^{n+1/2}, u^{n+1/2}, m_x^{n+1/2}, u_x^{n+1/2}\right), \tag{2.2}$$

where

$$m^{n+1/2} = \frac{1}{2}(m^{n+1} + m^n) \quad \text{and} \quad u^{n+1/2} = \frac{1}{2}(u^{n+1} + u^n). \tag{2.3}$$

It is known that the spatial accuracy of a numerical scheme depends on how accurately we can approximate the first-order derivative terms. In particular, if the equation of interest is a dispersive equation, such as Eq. (1.2), a dispersion-relation-preserving scheme is necessary to ensure the accuracy of numerical solutions. The first-order derivative terms $m_x^{n+1/2}$ and $u_x^{n+1/2}$ are approximated by a sixth-order dispersion-relation-preserving scheme developed by Chiu et al. [7] using the nodal values of (2.3). It is worth noting that the midpoint time integrator is a symplectic integrator [4,8], which retains the Hamiltonian invariants of the PDEs, if the spatially discretized PDEs are Hamiltonian systems. Since the evolution Eq. (2.2) is coupled with the Helmholtz equation, it is necessary to introduce an iterative scheme to obtain m^{n+1} and u^{n+1} from m^n and u^n. We do this by alternating between solving Eq. (2.2) and the Helmholtz equation, as described in the following steps:

- **Step 1**: Given an initial guess for $u^{n+1/2}$ and $m^{n+1/2}$, denoted $u^{(0),n+1/2}$ and $m^{(0),n+1/2}$ respectively, we solve the evolution Eq. (2.2) to obtain $m^{(1),n+1}$. The initial guess is based on Taylor series expansions:

$$\begin{aligned} m^{(0),n+1/2} &= 1.5m^n - 0.5m^{n-1}, \\ u^{(0),n+1/2} &= 1.5u^n - 0.5u^{n-1}, \end{aligned} \tag{2.4}$$

  where $n \geqslant 1$. When $n = 0$, we impose $m^{(0),1/2} = m_0$ and $u^{(0),1/2} = u_0$, where u_0 is the initial condition and $m_0 = u_0 - u_{0xx}$. Note that the initial guess (2.4) is chosen based on the facts that $t^{n+1/2} = t^n + \Delta t/2$, and the Taylor series expansions for $m(t^n)$ and $m(t^{n-1})$ about $t^{n+1/2}$ give

$$m(t^{n+1/2}) = 1.5m(t^n) - 0.5m(t^{n-1}) + O(\Delta t^2). \tag{2.5}$$

  Therefore, if we let $m^n = m(t^n)$ and $m^{n-1} = m(t^{n-1})$, the initial guess $m^{n+1/2}$ in (2.4) is an $O(\Delta t^2)$ approximation for $m(t^{n+1/2})$.
- **Step 2**: Using $m^{(1),n+1}$, we solve the Helmholtz equation to obtain $u^{(1),n+1}$. It is well known that in order to obtain a higher-order numerical method for the Helmholtz equation, one can always introduce more points in a stencil. The improved accuracy, however, comes at the cost of an expensive matrix calculation, due to the wider stencil. In this study, the Helmholtz equation is solved by a three-point sixth-order compact scheme developed in the paper by Sheu et al. [15]. We implement a multigrid method using the V-cycle and fully-weighted projection/prolongation with the red–black Gauss–Seidel smoother to solve the system of algebraic equations arising from the discretization.
- **Step 3**: Repeat **Step 1** and **Step 2** for the next iteration until the $(i+1)$th iteration, for which the residuals, in the maximum norm, of both Eq. (2.2) and the Helmholtz equation are less than our convergence criteria:

$$\begin{aligned} &\max_{x_j j=1,N} \left| \frac{m^{(i+1),n+1} - m^n}{\Delta t} - F\left(m^{(i+1),n+1/2}, u^{(i+1),n+1/2}, m_x^{(i+1),n+1/2}, u_x^{(i+1),n+1/2}\right) \right| \leqslant \varepsilon, \\ &\max_{x_j j=1,N} \left| m^{(i+1),n+1} - \left(u^{(i+1),n+1} - \alpha^2 u_{xx}^{(i+1),n+1}\right) \right| \leqslant \varepsilon, \end{aligned} \tag{2.6}$$

where N is the number of grid points, and the value for the threshold error ε is typically chosen to be 10^{-12} throughout our computations. Our numerical experiments indicate that the number of iterations needed for convergence with this value is less than 20 in general.

Note that for the equations

$$u_t = F(u, m_x), \quad m = u - \alpha^2 u_{xx}, \tag{2.7}$$

for example, coefficients $A = 0$, $B = 1$, $C = 0$, and $D = \alpha^2$ in (1.1), a similar iterative scheme is used in Section 4 to solve the evolution equation and the coupled Helmholtz equation.

We remark that in the paper by Chiu et al. [7], a two-step iterative algorithm (with the function F in the above algorithm as a special case) was employed to solve the shallow-water wave Eq. (1.2), a member of the class of PDEs considered in this study. Detailed error analysis for the dispersion-relation-preserving approximation as well as numerical convergence study

was carried out in that context, thanks to the availability of exact solutions. In addition, the von Neumann stability analysis was carried out in that paper to demonstrate the stability of the midpoint time integrator. These properties in principle do not depend on the specific equation and can be expected to hold for all equations in the class solved by the same principle of algorithm.

3. Numerical study of the regularized Burgers equation

Next, we turn our attention to numerical investigations of the regularized Burgers equation (1.3) and related equations. To this end, we provide several numerical examples to demonstrate:

1. For large α's, solutions of the regularized Burgers equation behave very differently from those of the Burgers equation with large viscosity ν.
2. For an arbitrary small α, solutions of the regularized Burgers equation could be significantly different from those of the Hopf equation at any finite time, even if the initial data are smooth or in a suitable function space as indicated in [1].
3. For any arbitrary small α, the longtime behavior of solutions of the regularized Burgers equation might be different from those of the Burgers equation with small viscosity ν.
4. The two third-order derivative terms uu_{xxx} and u_{xxt} produce high frequency oscillations individually when α approaches zero, but the dispersive effects cancel each other if the two terms appear together in an equation such as the regularized Burgers equation.

The following study aims at shedding some light on properties of this class of models. We begin our study with validating the two-step iterative algorithm for the regularized Burgers equation by comparing the result obtained by the proposed algorithm with that computed by the particle method developed in [6]. The method is based on turning to a Lagrangian form of Eq. (1.3), by which "particles" travel along characteristic curves of the regularized Burgers model, determined by solving a system of nonlinear integro–differential equations for the two variables q and p, which can be interpreted as the particle positions and momenta, respectively. This leads to the weak solutions of (1.3) which are the exact analog of "peakons" for the shallow-water equation. The integro-differential equations for q and p are expressed as follows:

$$\begin{aligned} q_t(\xi,t) &= \frac{1}{2\alpha}\int_{-\infty}^{\infty} \exp(-|q(\xi,t)-q(\eta,t)|/\alpha)p(\eta,t)d\eta,\\ p_t(\xi,t) &= -\frac{1}{2\alpha^2}\int_{-\infty}^{\infty} \operatorname{sgn}(\xi-\eta)\exp(-|q(\xi,t)-q(\eta,t)|/\alpha)p(\xi,t)p(\eta,t)d\eta. \end{aligned} \tag{3.1}$$

The velocity u can then be recovered from q and p as:

$$u(x,t) = \frac{1}{2\alpha}\int_{-\infty}^{\infty} \exp(-|q(\xi,t)-x|/\alpha)p(\xi,t)d\xi. \tag{3.2}$$

Discretizing the integro–integral Eq. (3.1) results in a finite dimensional dynamical system for "particles" with coordinates

$$q_i(t) \equiv q(\xi_i,t)$$

and momenta

$$p_i(t) \equiv p(\xi_i,t),$$

where $\xi_i = \Xi + ih$ for some real Ξ, step-size $h > 0$, and $i = 1,\ldots,N$. The finite dimensional system of ODEs for N particles for Eq. (3.1) can therefore be written as:

$$\begin{aligned} \dot{q}_i &= \frac{h}{2\alpha}\sum_{j=1}^{N} \exp(-|q_i-q_j|/\alpha)p_j,\\ \dot{p}_i &= -\frac{h}{2\alpha^2}p_i\sum_{i\neq j=1}^{N} \operatorname{sgn}(q_i-q_j)\exp(-|q_i-q_j|/\alpha)p_j. \end{aligned} \tag{3.3}$$

We will refer to system (3.3) as *the particle method* for solving the regularized Burgers Eq. (1.8).

3.1. Gaussian disturbance initial data

The first example we present here starts with a Gaussian disturbance initial data

$$u_0(x) = \frac{1}{5\sqrt{\pi}}\exp\left[-\left(\frac{x-50}{w}\right)^2\right], \tag{3.4}$$

where w is related to the initial width of the Gaussian disturbance. We choose the parameters $w = 20$ and $\alpha = 0.05$. Fig. 3.1(a) compares the evolution results by using the particle method and the two-step iterative algorithm. As demonstrated by the

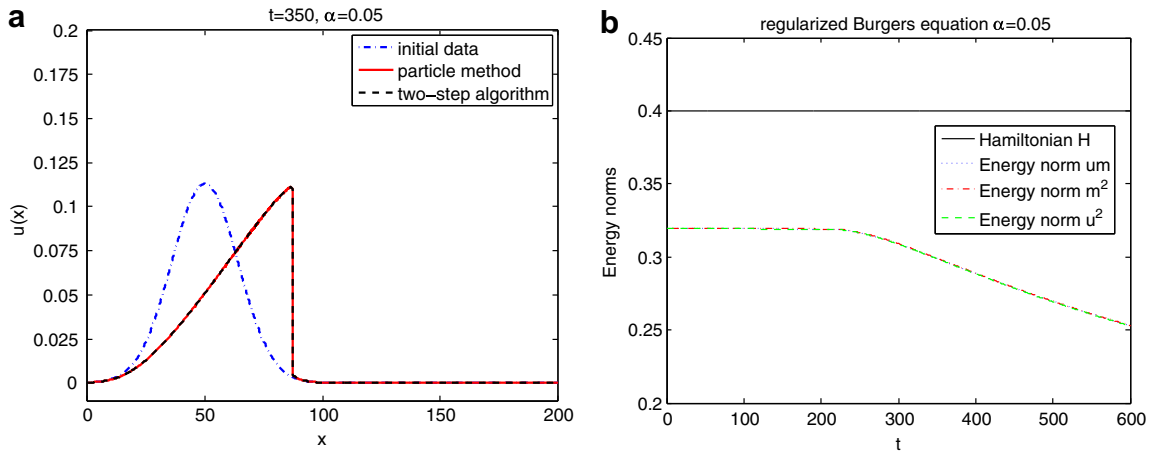

Fig. 3.1. An example taken from the paper by Mohseni et al. [13]. (a) Comparison of the particle method and the two-step iterative algorithm for the regularized Burgers equation with a Gaussian disturbance initial condition. (b) Plot of the energy norms and mass for the same equation and initial data in (a). For comparison, the value of mass (Hamiltonian) is divided by a factor 10.

figure, to within graphical accuracy the two independent numerical methods are identical. The number of grid points used in the two-step algorithm is $N = 20,481$ in the domain $[-50,250]$, while the number of particles used in the particle method is $N = 40{,}001$. The final time is $t = 350$. To further monitor the solution behaviors, we introduce mass H and the energy norms H_1, $L_2(m)$, and $L_2(u)$ as follows:

$$H = \int_{-\infty}^{\infty} u\,dx, \quad H_1 = \int_{-\infty}^{\infty} um\,dx, \quad L_2(m) = \int_{-\infty}^{\infty} m^2 dx, \quad L_2(u) = \int_{-\infty}^{\infty} u^2 dx. \tag{3.5}$$

Fig. 3.1(b) plots mass and the energy norms versus time and shows that mass is conserved, while all three energy norms decay almost at the same rate. In Fig. 3.2(a), we compare the numerical solutions of the Hopf and the regularized Burgers equations at final times $t = 350$ and $t = 600$. A similar comparison between solutions of the Hopf equation and that of the Burgers equation is shown in Fig. 3.2(b). We used $\alpha = 0.05$ in the regularized Burgers equation and $\nu = 0.015$ in the Burgers equation. Our calculations show that using the selected parameters, as time evolves the solution of the regularization Burgers equation follows the solution of the Hopf equation closely, instead of following the solution of the Burgers equation. In summary, our numerical experiments show that for single hump smooth initial data that are gently varying so that the second derivative of u is finite and small, solutions of the regularized Burgers equation with small α's follow those of the Hopf equation closely.

We remark that the same numerical calculations for the Gaussian initial data were performed in [13], and some discrepancies between our results and those presented therein can detected, possibly due to higher numerical viscosity from low

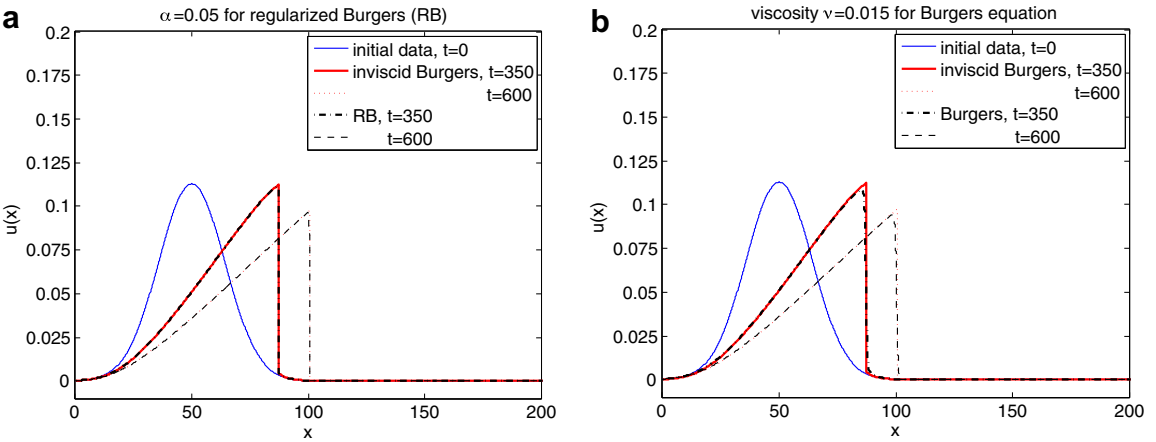

Fig. 3.2. The same example as Fig. 3.1. (a) Comparison of the solutions of regularized Burgers and inviscid Burgers (Hopf) equations at $t = 350$ and $t = 600$. (b) Comparison of the solutions of Burgers and inviscid Burgers (Hopf) equations at $t = 350$ and $t = 600$.

resolution. Finally, we remark that our numerical simulations for both the inviscid Burgers (Hopf) and Burgers equations in this section use the high-resolution finite volume method, CLAWPACK [12].

3.2. Nearly-square-wave initial data

Our next example is chosen to shed light on how solutions can evolve under the regularized Burgers equation starting from rough initial data. We consider the initial condition

$$u_0(x) = \frac{1}{2}\left(\tanh\left(\frac{x+15}{w}\right) - \tanh\left(\frac{x-15}{w}\right)\right), \tag{3.6}$$

where w is related to the width of the profile of the hyperbolic tangent function. When w is small, this is a nearly-square-wave initial data, with the narrowed smooth profiles centered at ±15. Note that the roughness parameter w is built-in and its independency of α brings substantially different features to the evolution than in the previous single hump example. We anticipate the possibility that non-uniform behavior in the limits of vanishing α and w can be expected, so that the inviscid regularization can lead unphysical evolution depending on (the class of) initial conditions, unlike its Burgers counterpart. A systematic physical derivation of the inviscid regularization might eliminate this possibility by requiring a link between initial data roughness and α when the latter is interpreted as a long wave parameter.

Fig. 3.3(a) shows solutions of the regularized Burgers equation with $\alpha = 0.05$ at final times $t = 5$ and $t = 10$, where $w = 0.01$ is chosen for the initial condition (3.6). The solutions are plotted against the Hopf equation. In contrast with the previous example, where the initial condition was a smooth Gaussian profile, the solution of the regularized Burgers equation emanating from the present initial condition follows that of the Hopf equation closely in the region of the right-propagating quasi-shock front, while the rarefaction wave region to the left exhibits markedly different behavior from the corresponding Hopf equation solution. The mechanism of such solution behavior is in fact better appreciated when looking at the finite dimensional dynamical system of the particle method developed in [6] for the regularized Burgers equation. We remark that in order to compare with the case of single hump initial data, the small parameter α used in this example is the same as that in the previous one. Fig. 3.3(b) shows the comparison between solutions of the Burgers equation and that of the Hopf equations. The solutions of the Burgers equation follow those of the Hopf equation closely, except for the smearing near the corners.

We perform simulations using the initial data (3.6) with various w's. Fig. 3.4 shows the solutions at $t = 0.1$ for $w = 0.05$ and 0.01, respectively. One can see that the left region of the wave grows into a hump almost immediately after the initial time. A similar phenomenon is reported in [2], where its connection to the smoothness of the initial data is analyzed. We note here that the amplitude of the hump depends on both w and the parameter α. Our numerical experiments indicate that as w decreases or α increases, the amplitudes of the humps also become larger. The mechanism of such a growth is related to the magnitude of the second derivative of u, which increases when w decreases. Hence for α fixed no matter how small, $m = u - \alpha^2 u_{xx}$ departs significantly from u. Notice that at the left corner of the nearly-square-wave, the second derivative of u is positive right before $x = -15$, and negative right after $x = -15$, hence m is negative before $x = -15$ and positive after $x = -15$. In [6], we show that such a structure is typical of a "peakon-antipeakon" solution, where m stretches and grows before some finite time. The implication of such a scenario is that in the limiting case when $w \to 0$, the left edge of the wave

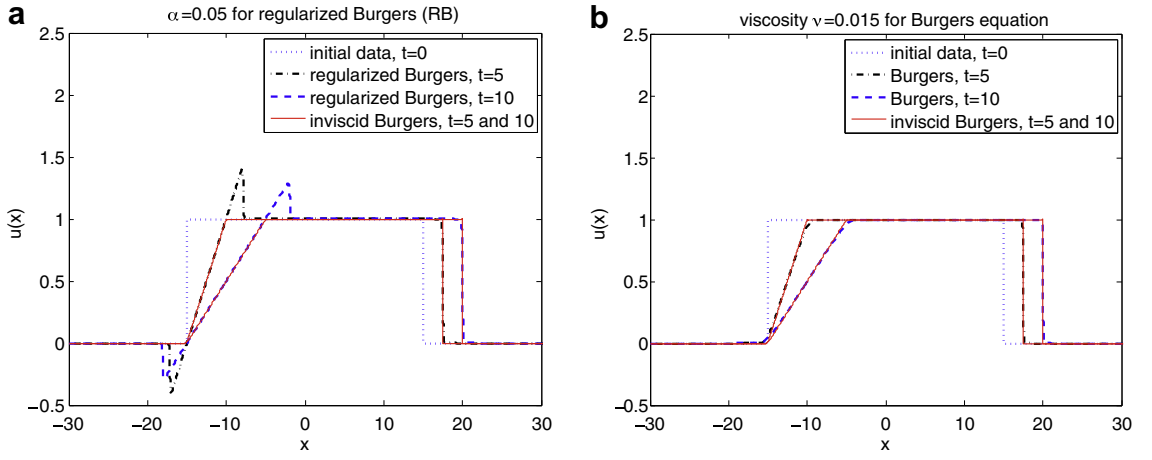

Fig. 3.3. A nearly-square-wave initial data, $w = 0.01$. (a) Comparison of the solutions of regularized Burgers and inviscid Burgers (Hopf) equations. $\alpha = 0.05$, the same as that used in [13] for the single hump initial data. Unlike the single hump initial condition, solutions of the two equations are different for this small α. (b) Similar to (a), comparison of the solutions of Burgers and inviscid Burgers (Hopf) equations. Viscosity $\nu = 0.015$, the same as that used in [13]. Solutions of these two equations are close.

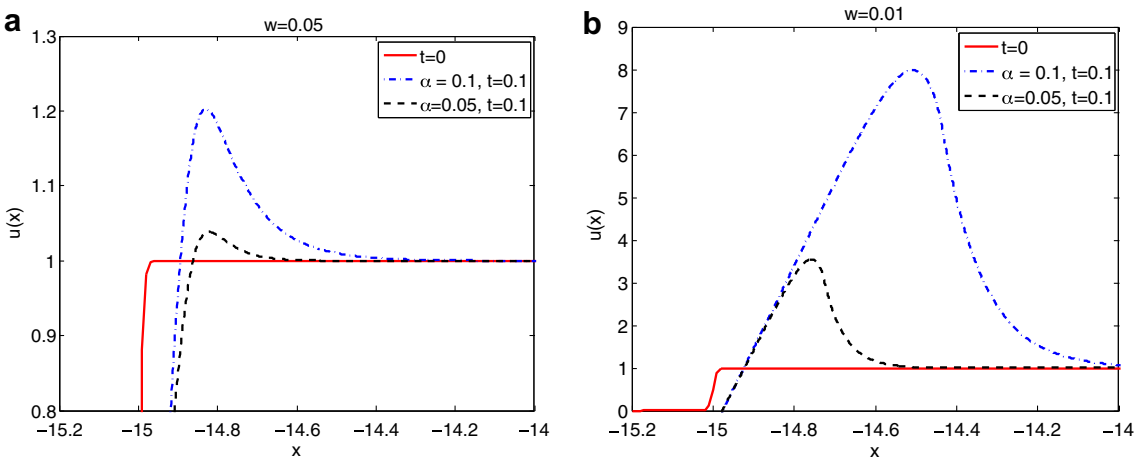

Fig. 3.4. Near square-wave initial data with different w in the hyperbolic tangent function. (a) $w = 0.05$, $\alpha = 0.1$ and 0.05. The solutions of the regularized Burgers equation are plotted at $t = 0.1$. The left-hand-side edge of the initial condition grows into a hump. The larger α's lead to larger growths of the hump. (b) The same calculation as (a), but $w = 0.01$ in the initial data. The bandwidth of the profile of the hyperbolic tangent function is much narrower in (b) than that in (a), and the growth of the hump is correspondingly larger.

might grow indefinitely for any fixed α. Based on a rescaling of the independent spatial variable with $w, \tilde{x} = x/w$, so that the Helmholtz operator becomes $1 - \alpha^2/w^2\,\partial_{\tilde{x}}^2$, one can see that a power law magnitude orderings between w and α might exist, for which the time scale when solutions of the regularized Burgers equation can be expected to behave like those of the Hopf equation can be made arbitrarily large. On the other hand, for the right edge of the initial data (3.6), we show in [6] that the particle method solution predicts that m decays, thus this edge does not exhibit any growth and the solution appears to be smeared out around the corners, just like solutions of the Burgers equation. Fig. 3.4 also indicates that for larger α's, the left edge of the initial data grows into larger humps. This of course is due to the contribution of second derivative of u due to larger α's. We notice that the number of grid points used for the two-step iterative algorithm is $N = 20{,}481$ in the domain $[-40, 40]$ for this example.

Note that adopting the alternative (Leray) viewpoint mentioned in the introduction, initial data $m(x,0) = m_0(x)$ that consist of a discontinuous sharp square-wave still can result into the growth of spikes in rarefaction waves, since the mollified velocity $u_0(x)$ of $m_0(x)$ can be viewed as equivalent to the nearly-square-wave initial data (3.6). However, we remark that in this formulation non-smooth initial data would require a shock-capturing scheme (such as ENO, WENO etc.) to avoid the numerical artifact of grid oscillations. Thus, a modification of the present algorithm would be required to pursue the evolution out of these classes of more singular initial data, unlike the case of Eq. (3.6) thanks to the smoothing of m_0 offered by such data.

3.3. Zero-mass initial data

An initial condition, such as

$$u_0(x) = \operatorname{sech}(x)\tanh(x), \tag{3.7}$$

has zero-mass. It was shown in [16] that for this type of zero-mass initial data (negative mass at the left and positive mass at the right), solutions of the Burgers equation with small viscosity evolve into the so-called N-wave structure in some finite time. As time further evolves, the diffusion eventually dominates the nonlinear term in the final decay, no matter how small the viscosity is. This final time period of decay, however, occurs at increasingly larger times as $\nu \to 0$. Such a phenomenon is confirmed numerically in [3] using the technique of renormalization group. Fig. 3.5(a) shows the comparison of the solutions of Hopf and Burgers equations with viscosity $\nu = 0.015$ at $t = 80$. With this small viscosity, the solution of the Burgers equation maintains the N-wave structure, except at the corners which are smeared out by viscosity.

Similarly, using $\alpha = 0.05$, in Fig. 3.5(b) we show the solution of the regularized Burgers equation at $t = 80$, plotted against the solution of the Hopf equation. One can see that at $t = 80$ solutions of the two equations are visually identical. At larger times, the diffusion in the Burgers equation is expected to dominate the solutions. The long time behavior of the regularized Burgers equation from these initial data as α decreases seems to pose an interesting question which is currently under investigation using the technique of renormalization groups. Here we present some numerical results, where in order to compare with the single hump initial condition example, we choose the same values of ν and α as those in the first example. The aim is that of comparing properties of the third derivative terms and the diffusion term for zero-mass initial data. We perform simulations for the Burgers and the regularized Burgers equations using both large and small ν's and α's. When viscosity is large, the diffusion term in the Burgers equation dominates the nonlinear term. One can observe that solutions of the Burgers

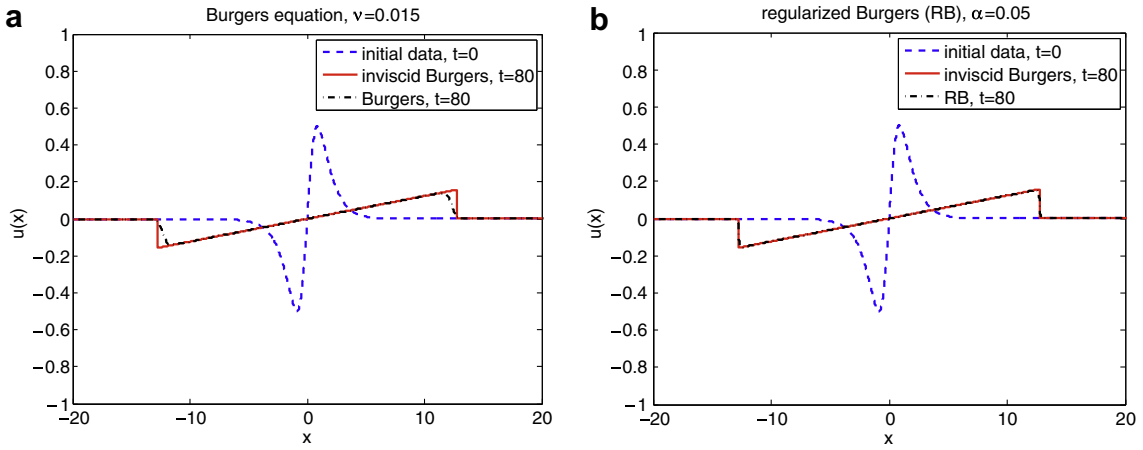

Fig. 3.5. A zero-mass initial data. Viscosity used in the Burgers equation and the parameter α used in the regularized Burgers equation in this example are the same as those in previous examples. (a) Comparison of the solutions of Burgers and inviscid Burgers (Hopf) equations at $t = 80$. Both solutions have the N-wave structure. (b) Comparison of the solutions of regularized Burgers and inviscid Burgers (Hopf) equations at $t = 80$. The two solutions are almost identical.

equation dissipate into something similar to the dipole solution of the heat equation at early times. Fig. 3.6 shows the comparison of the solutions of Hopf, Burgers, and regularized Burgers equations at $t = 80$. The parameters are $\nu = 1$ and $\alpha = 1$. Inset of Fig. 3.6 shows the magnification of solutions of the Burgers equation with viscosity $\nu = 1$ at $t = 80$, which demonstrates how the solution no longer exhibits an N-wave structure and instead is close to a dipole solution of the heat equation.This simulation suggests that when ν and α are both large, solutions of the Burgers and the regularized Burgers equations depart from those of the Hopf equation for zero-mass initial data. Solutions of the Burgers equation are expected to be heavily dissipated and lose the N-wave structure at a fairly early stage, whereas solutions of the regularized Burgers equation maintain the N-wave structure, but with a larger amplitude and wave speed than those observed for the Hopf equation.

In the next simulation, we demonstrate the difference between the Burgers and the regularized Burgers equations for the zero-mass initial condition, when both ν and α increase. Fig. 3.7(a) are solutions of the Burgers equation for viscosity increasing from $\nu = 0.5, \sqrt{0.5}$, to 1 at the final time $t = 4$. The dotted line is the initial data. As expected, the initial data gets dissipated, and the dissipation gets larger when viscosity gets larger. Fig. 3.7(b) shows solutions of the regularized Burgers equation at the same finial time for $\alpha = 0.5, \sqrt{0.5}$, and 1. In contrast to (a), the initial amplitude grows with time, and the amplitude of growth increases with increasing α.

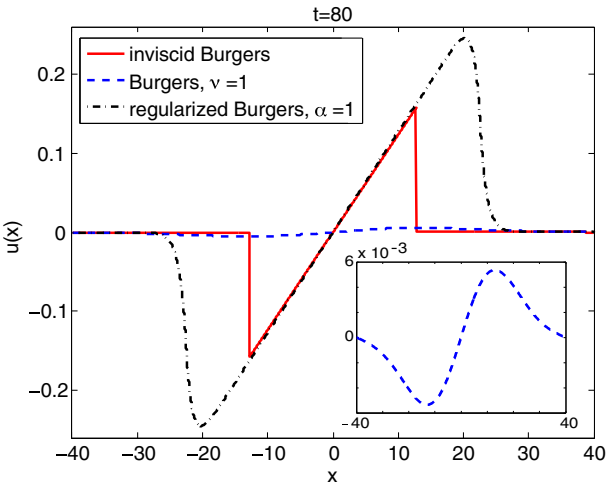

Fig. 3.6. The initial data is the same as Fig. 3.5, but viscosities and the parameter α used in the equations are bigger. Comparison of the solutions of Burgers, regularized Burgers, and inviscid Burgers (Hopf) equations. $\nu = 1$ in the Burgers equation and $\alpha = 1$ in the regularized Burgers equation. Inset shows the solution of the Burgers equation at $t = 80$ for viscosity $\nu = 1$. The solution is similar to the dipole solution of the heat equation. The solution of the regularized Burgers equation maintains the N-wave structure, but the amplitude is much bigger and the wave speed is also faster than those of the inviscid Burgers (Hopf) equation.

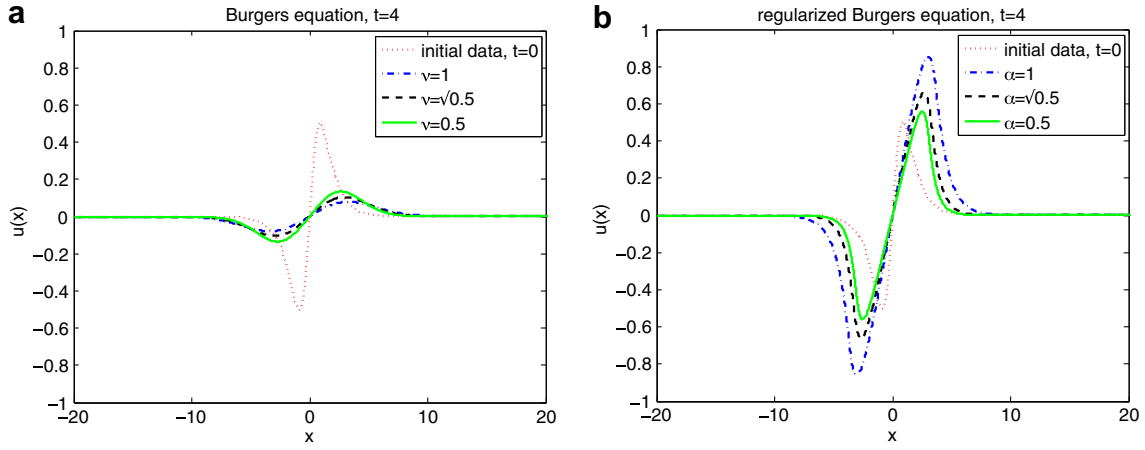

Fig. 3.7. The same initial data as Figs. 3.5 and 3.6. (a) Solutions of the Burgers equation. Viscosity increases from 0.5, $\sqrt{0.5}$ to 1. The initial data gets dissipated, and the dissipation gets larger when viscosity gets larger. (b) Solutions of the regularized Burgers equation. The parameter α also increases from 0.5, $\sqrt{0.5}$ to 1. The initial amplitude grows with time, and the amplitude of growth increases with increasing α.

Finally, we comment on the time steps and the boundary conditions chosen for the above numerical examples. For our numerical examples, if the choice of time step is not specified, a fixed time step Δt is chosen to be

$$\frac{c\Delta t}{\Delta x} \leqslant \frac{1}{2}, \tag{3.8}$$

where Δx is the grid size and c is some constant that is independent of Δt or Δx. For the boundary conditions, since the functions of numerical examples illustrated in this section decay rapidly before the boundaries, we use periodic boundaries for all calculations. The domains are chosen to be large enough so that waves would not reach the boundaries before the final time of calculation.

4. Physical insights of the role of uu_{xxx} and u_{xxt} in the regularized equation

Having gained some knowledge about the solution behavior of Eq. (1.3), we now focus our attention on the interplay between the two third derivative terms, $u\,u_{xxx}$ and u_{xxt}. Our numerical investigation aims at providing information for future analysis of the Helmholtz-type regularization.

It was pointed out in [1] that the regularized Burgers equation (1.3) is the $b = 0$ member of the b-family described in [9]

$$m_t + um_x + bu_x m = 0. \tag{4.1}$$

All equations in the b-family are also in the class of PDEs we consider ($A = 1$, $B = b$, $C = 0$, $D = 0$, and $K = 0$ in Eq. (1.1)) and hence can all be solved using the proposed two-step iterative algorithm in this paper.

With one of the third derivative terms missing in the regularized Burgers equation, we expect that the BBM equation, (1.11) or (1.12), and the dispersive equation, (1.9) or (1.10), to behave totally differently from the regularized Burgers equation as $\alpha \to 0$. We compare the regularized Burgers equation and these two equations when α approaches zero for a single hump initial condition. Consider the initial condition

$$u_0(x) = \operatorname{sech}(x), \tag{4.2}$$

in the domain of $-10\pi \leqslant x \leqslant 10\pi$. The breaking time of the Hopf equation for this initial condition is

$$t_b = -1/\min(u_x(x,0)) \cong 2.$$

After this time, the Hopf equation no longer has classical solutions for these initial data. Hence we choose the final time $t = 8$, long after the shock has to be fitted for the Hopf solution, for the simulations of the regularized Burgers equation (1.8), the BBM equation (1.12), and the dispersive Eq. (1.10). Similar to the $b > 0$ case in the b-family, we expect that the zero-α limit is a zero-dispersion limit for both Eq. (1.10) and the BBM equation (1.12). Fig. 4.1 shows simulations for the BBM and the dispersive equations. The results are compared with the regularized Burgers equation. The left-hand-side column is the dispersive Eq. (1.10) and the right-hand-side is the BBM equation (1.12). From top to bottom, the parameter α is 0.1, 0.01, and 0.001 respectively. The dashed line is the regularized Burgers equation. One can clearly detect that when α decreases the frequency of oscillations increases for both equations, but the oscillations cancel each other when both the third-order derivative terms appear in the equation. The cancellation is expected, since the regularized Burgers equation is not a dispersive equation. However it is numerically impossible to test whether the balance between these terms is maintained indefinitely in time.

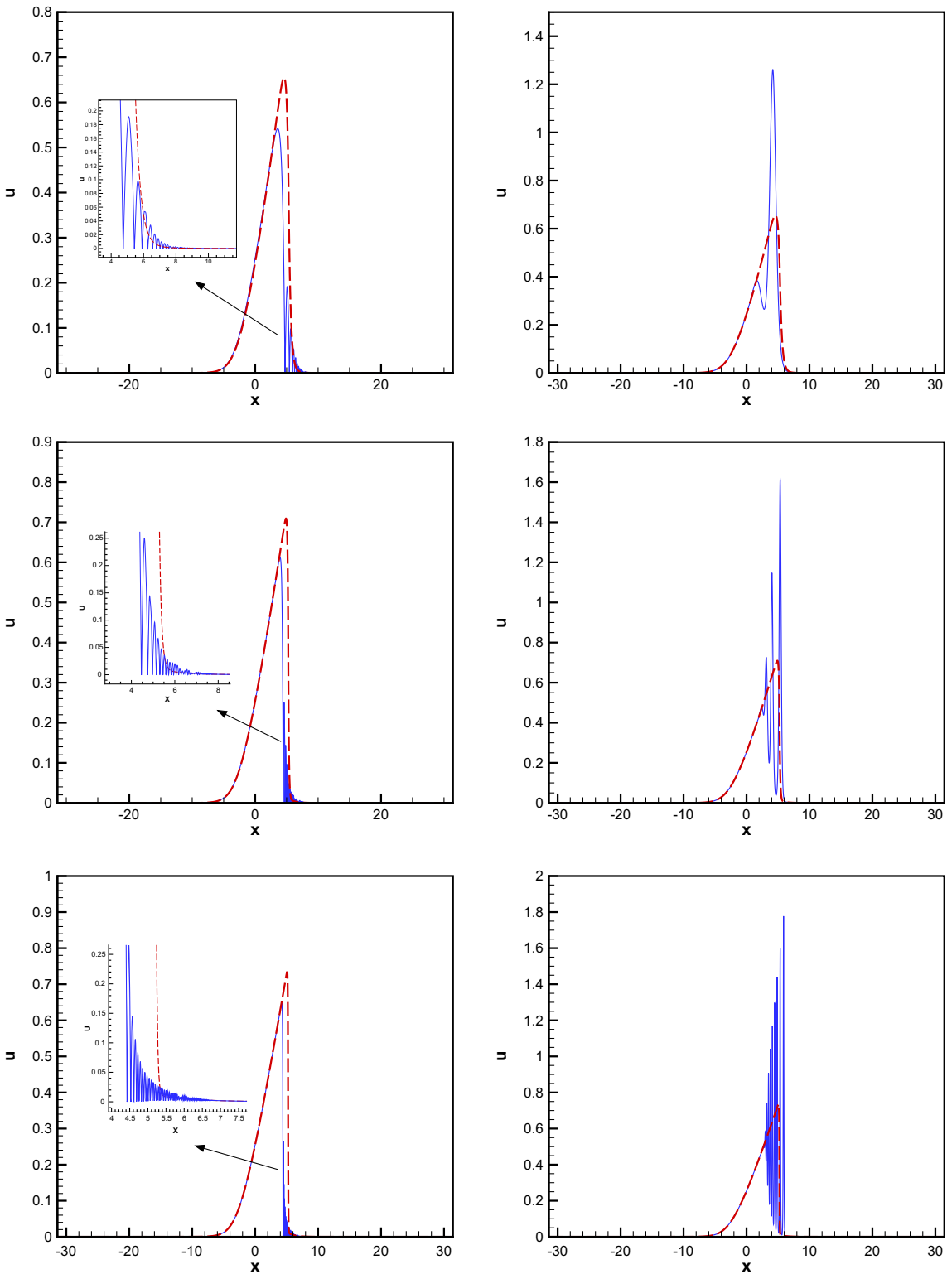

Fig. 4.1. The left-hand-side column is the dispersive Eq. (1.10) and the right-hand-side is the BBM equation (1.12). From top to bottom, the parameter α is 0.1, 0.01, and 0.001 respectively. The dashed line is the solution of regularized Burgers equation.

The number of grid points used in these simulations is $N = 8193$. It is worth noting that we perform grid refinement study for this example. Simulations by using finer grids are almost the same as those presented in Fig. 4.1.

5. Discussion and conclusion

In this study, we employ a two-step iterative scheme for solving a class of PDEs involving the Helmholtz operator. We investigate solution properties of members of this class of PDEs, including the regularized Burgers equation and two dispersive equations whose structure is reminiscent of physically relevant models of shallow-water wave propagation such as BBM and KdV. Interestingly, these models arise from selecting one term between the two that comprise the Leray-type regularization. Our numerical investigation indicates the follows:

1. For large α's, solutions of the regularized Burgers equation behave very differently from those of the Burgers equation with large viscosity ν.
2. For an arbitrary small fixed α, solutions of the regularized Burgers equation could still be significantly different from those of the Hopf equation at any finite time, even if the initial data are smooth or in a suitable function space as in [1].
3. For any arbitrary small fixed α, the longtime behavior of solutions of the regularized Burgers equation might be different from those of the Burgers equation with small fixed viscosity ν.
4. The two third-order derivative terms uu_{xxx} and u_{xxt} produce high frequency oscillations individually when α approaches zero, but these dispersive effects cancel each other out if these two terms appear together as in the regularized Burgers equation.

For these reasons, it appears that the inviscid regularization requires extra care in its application with respect to its standard Burgers counterpart, and in particular it should not be applied outside of a systematic derivation that assigns a physical meaning to the limit of vanishing α with respect to the initial data. While we clarify some issues of the regularized Burgers equation and two related equations, there still are several questions that are not answered in this study regarding the employed method and other solution properties of the equations. These are currently under investigation.

1. The two-step iterative method employed in this study is somewhat reminiscent of operator splitting methods, though we couple this with an iteration with a stoppage threshold criterion. It is not clear what splitting error is introduced by solving the two equations in alternating fashion. We are developing an a posteriori error estimator to evaluate the splitting error introduced by the iterative scheme.
2. The dispersive effects by the two third-order derivative terms, u_{xxt} and uu_{xxx}, cancel each other when the two terms appear together in the equation, but it is not clear if one of the two terms dominates at extremely long times. This is inherent to the question on the longtime behavior of the regularized Burgers equation with zero-mass initial conditions, for fixed (small) α. This question is under investigation using the technique of renormalization group.
3. Our numerical example shows that when the second derivative of an initial condition is extremely large at some points, no matter how small the parameter α is, solutions of the regularized Burgers equation are different from those of the Hopf equation, as well as those of the Burgers equation with small viscosities. The evolution of solutions of the regularized Burgers equation for rough initial data is an open question, and the present investigation only suggests possible scenarios for step-like data.

Acknowledgements

This research is partially supported by NSF through Grant DMS-0610149 (LL) and DMS-0509423 (RC). T.W.H. Sheu would like to thank the Department of Mathematics at the University of Wyoming for its provision of excellent research facilities during his visiting professorship.

References

[1] H.S. Bhat, R.C. Fetecau, A Hamiltonian regularization of the Burgers equation, J. Nonlinear Sci. 16 (2006) 615–638.
[2] H.S. Bhat, R.C. Fetecau, The Riemann problem for the Leray–Burgers equation, J. Differ. Equ. 246 (2009) 3957–3979.
[3] G.A. Braga, F. Furtado, V. Isaia, Renomalization group calculation of asymptotically self-similar dynamics, Proceeding of the Fifth International Conference on Dynamical Systems and Differential Equations, June 16–19, 2004, Pomona CA, USA, pp. 1–13.
[4] J.D. Brown, Midpoint rule as a variational-symplectic integrator: Hamiltonian systems, Phys. Rev. D 73 (024001) (2006) 1–11.
[5] R. Camassa, D. Holm, An integrable shallow water equation with peaked solitons, Phys. Rev. Lett. 71 (1993) 1661–1664.
[6] R. Camassa, P.H. Chiu, L. Lee, T.W.H. Sheu, A particle method and numerical investigation of a Helmholtz regularization of the Burgers equation, DCDS-S, in press. Available upon request to <http://llee@uwyo.edu>.
[7] P.H. Chiu, L. Lee, T.W.H. Sheu, A dispersion-relation-preserving algorithm for a nonlinear shallow-water wave equation, J. Comput. Phys. 228 (2009) 8034–8052.
[8] J. De Frutos, J.M. Sanz-Serna, An easily implementable fourth-order method for the time integration of wave problems, J. Comput. Phys. 103 (1992) 160–168.
[9] A. Degasperis, D.D. Holm, A.N W. Hone, Integrable and Non-Integrable Equations with Peakons, Nonlinear Physics: Theory and Experiment–II, World Scientific Publishing, River Edge, NJ, 2003. pp. 37–43.
[10] R.S. Johnson Camassa-Holm, Korteweg-de Vries and related models for water waves, J. Fluid Mech. 455 (2002) 63–82.
[11] J. Leray, Sur le mouvement d'un liquide visqueux emplissant l'espace, Acta Math. 63 (1934) 193–248.
[12] R.J. LeVeque, Finite Volume Methods for Hyperbolic Problems (Cambridge Texts in Applied Mathematics), first ed., Cambridge University Press, 2002.

[13] K. Mohseni, H. Zhao, J. Marsden, Shock regularization for the Burgers equation, in: AIAA Paper 2006–1516, 44th AIAA Aerospace Science Meeting and Exhibit Reno, Nevada, January 9–12, 2006.
[14] G. Norgard, K. Mohseni, A regularization of the Burgers equation using a filtered convective velocity, J. Phys. A: Math. Theor. 41 (344016) (2008) 21.
[15] T.W.H. Sheu, L.W. Hsieh, C.F. Chen, Development of a three-point sixth-order Helmholtz scheme, J. Comput. Acoust. 16 (2008) 343–359.
[16] G.B. Whitham, Linear and Nonlinear Waves (Pure and Applied Mathematics: A Wiley Series of Texts, Monographs and Tracts), Wiley-Interscience, 1999.